Applied Physics Research; Vol. 16, No. 1; 2024
ISSN 1916-9639 E-ISSN 1916-9647
Published by Canadian Center of Science and Education

Development of Patented Autonomous Quantum Gravitational Electric Energy Generator Prototypes

Claude Poher[1] & Danielle Poher[1]

[1] Laboratoire Aurora, F31400, Toulouse, France

Correspondence: Claude Poher, Laboratoire Aurora, F31400, Toulouse, France. E-mail: claude.poher@wanadoo.fr

Received: December 23, 2023 Accepted: January 15, 2024 Online Published: February 14, 2024

doi:10.5539/apr.v16n1p64 URL: https://doi.org/10.5539/apr.v16n1p64

Abstract

After quantum physics modelling of Gravitational interaction from hypotheses, we performed experimental confirmation experiments of predicted increased Faraday's induction. Brief and low energy electric discharges were made, at room temperature, into partially superconducting Graphite based devices, patented and named "emitters", inserted in series with the primary low inductance of a transformer. The high voltage secondary inductance of that transformer was connected to a capacitor, so the secondary current oscillated during several milliseconds.

We Measured the global energy efficiency of Faraday's induction, during each electric discharge into the emitter of the primary circuit. We also measured evolution of the peak primary discharge current, and of its derivative, versus the initial charge voltage. We observed systematically a much larger than 100% energy efficiency. That energy efficiency increases with the primary discharge energy. The peak discharge current is observed to be much larger than predicted by Ohm's Law, and the discharge current derivative is also observed to be much larger than classically predicted.

Same experiments, performed with "normal conductive devices (control)", gave energy efficiencies much lower than 100 %, independent of the stored energy. And their peak discharge currents and derivatives followed Ohm's Law.

From these confirmations of predicted results, we proposed and tested successfully concepts of Autonomous electric Generators prototypes, extracting their energy from the cosmological Gravitational quantum field. Their industrial use into electric vehicles should preserve Earth fossil energy resources, as well as reduce the detrimental climate effects of greenhouse gases emissions. Hypotheses are suggested to explain the observed experimental facts.

Keywords: energy generation, quantum gravitation, superconductors, Faraday's induction

1. Introduction

Being officially in charge of international space astronomical experiments of France into CNES (Centre National d'Etudes Spatiales), during the 1970's, corresponding author was concerned by discovery of the unmodelled behavior of Gravitation revealed into spiral galaxies by Vera Rubin's Group, giving rise to the yet unproven hypothesis of "Dark matter" [Rubin, 1995, 12].

We tried to find another potential explanation than dark matter. To do this, from quantum physics theoretical hypotheses, we get progressively in 2002, a quantum model of the gravitational interaction we published only in 2020 [Poher, 2020, 3]. This late publication was required, as hypothetic and controversial gravitational Quanta used and named "Universons" did not had the attractive characteristics of "Gravitons", the concept coined in 1934 by Blokhintsev. Effectively, hypothetic Universons bear a positive tiny momentum $Pu = 2.8.10^{-31}$ kg.m/s (so they have a pushing action on matter) and interact with massive elementary particles of matter with a specific Quantum behavior which seems to look like a phase inversion of their wave function.

Before publishing such a hypothetic model, it was effectively first required to get experimental confirmations of its predictions. These were confirmed and published in 2011 [Poher, 2020, 3] along with the many physical effects observed, thanks to the patented invention of diverse superconducting electric "***emitters***" of artificial gravitational

field [Poher, 2006, 1], [Poher, 2020, 5]. These emitters contained many Josephson Junctions, into which electrons were strongly accelerated.

We pursued experimentally along 15 years the study of physical phenomena revealed by the interaction of our patented emitters with the natural Quantum Gravitational field.

From thousands of experiments performed along that period, we confirmed that, during brief electric discharges into the emitters, there is mainly a systematically strong propelling effect of that devices, without ejection of matter [Poher, 2011, 2], and also there is systematically a strong increase of Faraday's induction into distant coils [Poher & Modanese, 2017, 4].

Such experimental results were observed first with YBCO based emitters, immersed into liquid nitrogen [Poher, 2006, 1], [Poher 2011, 2], then, since 2015, with Graphite based superconducting emitters used at room temperature, according to [Poher, 2017, 4], [Esquinazi, 2012, 7].

We modeled these phenomena and improved our experimental systems [Poher, 2017, 4] of distant Faraday's induction, using low losses miniature transformers, with nano-crystalline soft magnetic material, giving larger output voltages, in order to confirm our theoretical predictions of larger than 100 % energy efficiencies.

This has given rise to the development of Quantum Autonomous electric Gravitational generators prototypes.

2. Experimental Setup and Methods

2.1 Principle of Our Basic Augmented Faraday's Induction Experiments

The basic circuit consists of a transformer (Figure 2) made of a "Finemet" C-Core nano-crystalline soft magnetic material, having low losses at current oscillations frequency (≃7500 Hertz). The Core has a total width of 125 mm, and a total air gap of 400 microns.

Three inductances made the transformer (Figure 1). The primary coil L1 has a single turn, it is part of the primary discharge circuit L1 C1. Capacitor C1 (206.5 µF, insulated to 4 kV) is first charged at a DC voltage Uo chosen between 40 and 100 Volts, from an external adjustable DC power supply.

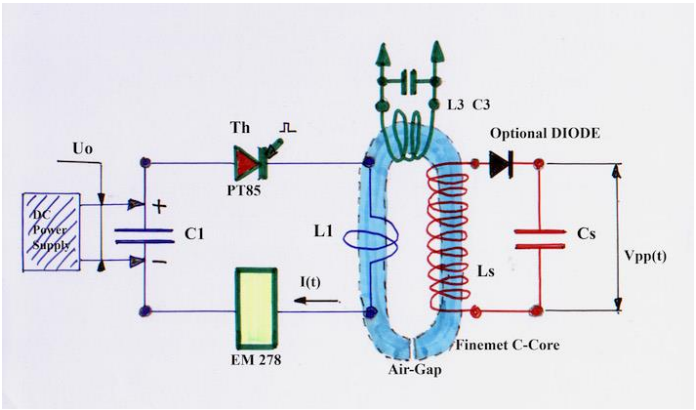

Figure 1. Electric circuit used during basic confirmation experiments

Capacitor C1 is discharged into L1, trough the negligible internal resistance oversized GTO thyristor PT85, controlled manually, and through the Graphite based emitter device EM278 whose DC resistance is of the order of 0.02 Ohm. That primary circuit is under-damped by the low emitter internal resistance, therefore it does oscillate very briefly during electric discharges, the anti-parallel internal diode of the GTO thyristor allows this.

Secondary transformer coil Ls has 111 turns, it is connected to a capacitor Cs (23.8 nF insulated to 36 kV). That secondary circuit oscillates during electric discharges into the primary circuit. The "optional" Diode was not used (shorted) during first experiments described here, its role will be explained later about the concept generator application.

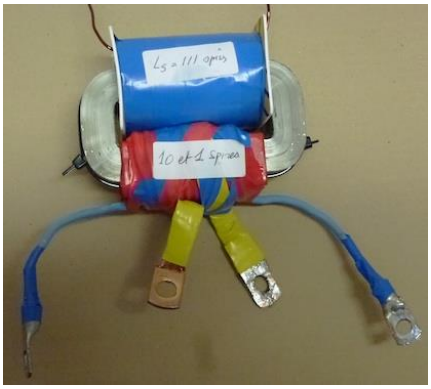

Figure 2. Finemet C-Core material transformer, with 400 µm Air-Gap, and three coils, before its installation into the experimental circuit and oil immersion. Its maximum potential power is about 10 KVA.

The recharging role of the third oscillating circuit L3 C3 (10 turns for L3, and 0.463 µF for C3, insulated to 1500 Volts) will also be described later. It was not used during the first experiments (C3 disconnected).

During functional tests, L1 C1 = Ls Cs = L3 C3. Measured inductances values at 1kHz and low current are: L1 (one turn) = 2.5 µH. Ls (111 Turns) = 15.451 mH. L3 (10 turns) = 144.8 µH. Theoretical low current oscillation frequency of Ls Cs = 7576 Hz.

Figure 3. Transformer, capacitor C3, and 1/100 M frequency compensated voltage divider, bolted on a PTFE insulating platform, ready for oil immersion required to avoid Corona discharges.

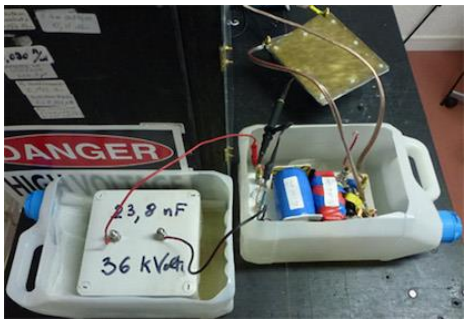

Figure 4. Transformer and capacitor Cs installed into separate containers for immersion into mineral oil. Emitter EM278 and remaining of the low voltage discharge circuit were not immersed.

Capacitor Cs (Figure 4) and the transformer (Figure 3) must be immersed into mineral oil to avoid Corona discharges at the large induced voltages (up to 30 kV). Capacitor C1, the thyristor and emitter EM278 remain

outside oil bath because submitted to voltages lower than 100 volts. We did not at first performed the required vacuum oil impregnation of coils wires and capacitor plates therefore tiny air bubbles remained present.

2.2 Partially Superconducting Emitter

Patented emitter EM278 has two square brass electrodes (200 mm sides and 2 mm thickness each). They squeeze a paste made of Graphite grains (Figures 5 & 6), according to recommendations of the Leipzig University Group [Esquinazi, 1999, 6], [Esquinazi, 2012, 7] & [Esquinazi, 2019, 8]. That paste contains several superconducting zones, where should exist Cooper pairs of electrons. We added ingredients into that paste, able to create millions of randomly oriented Josephson Junctions where the material was superconducting [Josephson, 1974, 9].

Figure 5. Graphite based paste spread onto one of the two brass electrodes of EM278, surrounded by two peripheral joints, between which are inserted the insulated 12 brass assembly bolts.

Figure 6. The lower brass electrode of emitter is pressed onto the Graphite paste and peripheral bolts are secured. There is a fastening soldered central brass 8 mm screw, as it auto-propels during electric discharges. Each electrode has a triangular “appendix”, with 6 mm hole, for electrical connection.

2.3 Storage Capacitor C1 and PT85 GTO Thyristor Installation

Figure 7. Full configuration, with immersion in mineral oil. The rear black insulated box contains capacitor C1 and PT85 GTO thyristor, with its command circuit. Capacitor Cs is connected through high voltage cables

An oversized 206.5±0.1 μF energy storage capacitor C1 insulated to 4000 Volts is used, its size is much larger than the immersed transformer. Oversized GTO thyristor PT85 is also insulated to 4000 Volts with 20000 peak Amperes capability. These were used for other kinds of higher power experiments. Both are installed into an

insulated box (Figure 7). Command of the thyristor conduction is obtained through an electronic circuit, delivering a calibrated 180 µs long electric pulse duration on manual command.

2.4 Data Measurement and Recording

Charge voltage Uo of capacitor C1 is delivered by a separate DC power supply, and Uo value is known from a four digits voltmeter (Figure 7) with an accuracy of ± 1 Volt. Discharge current is measured via a Tektronix oscilloscope, and Rogowski probe, installed close to the PT85 thyristor, into the insulated black box. The probe is calibrated from a professional similar instrument. Its calibration factor is 4.08 Amperes per output millivolt. Its bandwidth at – 6 dB is 100 kHz. Induced voltage into secondary inductance Ls is measured trough two successive attenuators. The first one, frequency compensated, of ratio 1/100 M is immersed into mineral oil. The second one, also of ratio 1/100, is the oscilloscope probe. The total attenuation is 1/10000. The oscilloscope shows amplitudes on its screen with a maximum ratio of 1/1000, therefore we have to multiply its indications for Vpp or Peak induced voltage (blue curves) by 10.

Tektronix oscilloscope used allowed recording digitally its screen image onto a USB key as a jpg format file. Our observations were made at a time scale of 100 µs per division (900 µs full screen width). The oscilloscope bandwidth (40 MHz) was much larger than the frequency of the involved signals (7.5 kHz).

Let us consider a typical set of measured parameters during an electric discharge trough the emitter.

3. Example Results

3.1 Four Discharges Examples Measurements and Comments

3.1.1 Discharge With Uo = 40 Volts (0.17 Joule)

- Peak Current = 183 Amperes.
- Peak to peak output voltage Vpp = **14400 Volts**.
- Peak negative charge of Cs Vp = **— 8000 Volts**. Vp is the large amplitude second alternation.
- Oscillating frequency = 7576 Hertz.
- Recorded on file TEK0045.jpg. (Figure 8).
- Energy efficiency: h = Cs / C1 (Vp / Uo) ^{2} = **460 %**.

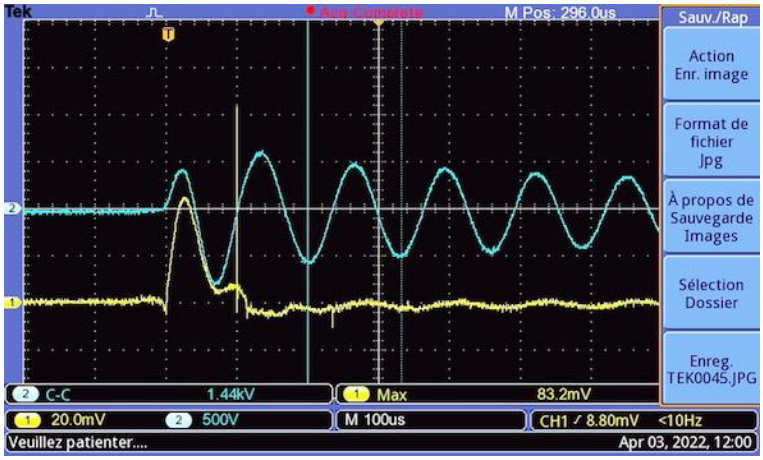

Figure 8. Discharge with Uo = 40 Volts. Yellow curve = discharge current (81.6 Amperes per division). Blue curve = induced voltage Vpp (**5000 Volts per division**). **Time scale = 100 µs per division**. Spikes on Chanel #1 were caused by Corona discharges into remaining confined air bubbles.

3.1.2 Comments About Previous Discharge With Uo = 40 Volts

The few brief "spikes" onto the discharge current yellow curve, are indications of Corona discharges into air bubbles confined inside oil immersed components. Effectively air is ionized at about 2500 Volts per millimeter electric field. This consumes energy.

Moreover, the discharge current wave shape is not “classical” for a capacitor discharge, it oscillates after the 180 µs duration of thyristor command pulse. This probably because of the conduction of the antiparallel Diode of the GTO thyristor. This consumes also energy by retro-induction from the secondary current towards the primary circuit. Nevertheless, the energy efficiency calculated for the largest amplitude negative alternation is four times larger than 100 %.

The different identified losses reduce the oscillating peak to peak induced voltage amplitude of the Ls Cs circuit, however 300 µs after the discharge beginning, the peak to peak oscillating voltage remains quite large (**10000 Volts**) with a symmetric wave shape, and a remaining **energy efficiency of 180 %.**

This means 400 – 180 = 220 % electric energy losses.

Clearly, the discharge current derivative is quite large, we will measure it.

3.1.3 Discharge With Uo = 60 Volts (0.37 Joule)

- Peak Current = 290 Amperes.
- Peak to peak output voltage Vpp = **22400 Volts**.
- Peak negative charge of Cs Vp = **— 12600 Volts**.
- Oscillating frequency = 7812 Hertz.
- Recorded on file TEK0043.jpg. (Figure 9)
- Energy efficiency: h = Cs / C1 (Vp / Uo) ^{2} = **508 %**.
- Energy efficiency 300 µs later = **119 %. Energy losses = 508 – 119 = 389 %.**

There are manifestly larger losses than during Uo = 40 Volts discharge, particularly by retro-induction.

We should have not used a GTO thyristor for the discharges. The primary current wave shape is eloquent

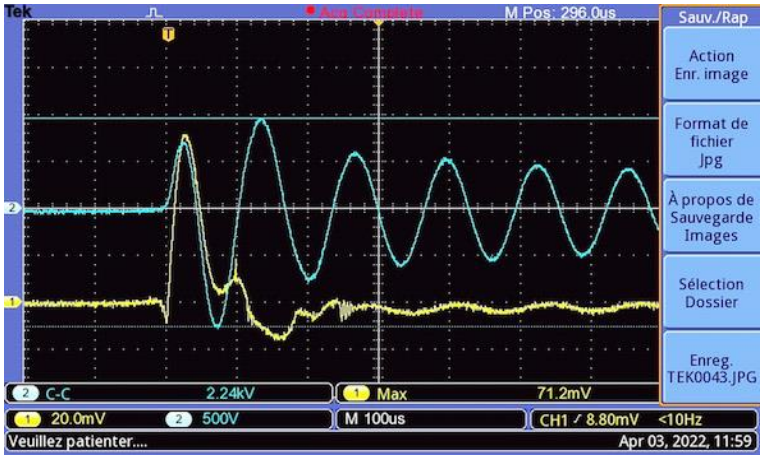

Figure 9. Discharge with Uo = 60 Volts. Yellow curve = discharge current (81.6 Amperes per division). Blue curve = induced voltage Vpp (**5000 Volts per division**). **Time scale = 100 µs per division**.

3.1.4 Discharge with Uo = 80 Volts (0.66 Joule)

- Peak Current = 408 Amperes.
- Peak to peak output voltage Vpp = **35800 Volts**.
- Peak negative charge of Cs Vp = **— 24000 Volts**.
- Oscillating frequency = 7576 Hertz.
- Recorded on file TEK0047.jpg. (Figure 10).
- Energy efficiency: h = Cs / C1 (Vp / Uo) ^{2} = **1037 %**.

— Energy efficiency 300 µs later = **51 %. Energy losses = 1037 – 51 = 986 %.**

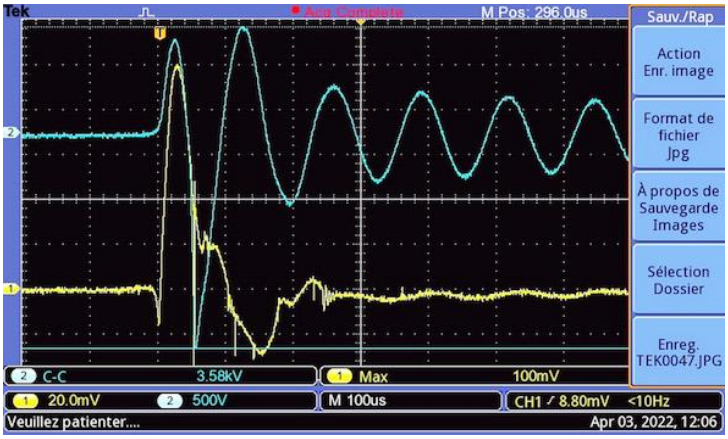

Figure 10. Discharge with Uo = 80 Volts. Yellow curve = discharge current (81.6 Amperes per division). Blue curve = induced voltage Vpp (5000 Volts per division). Time scale = 100 µs per division.

There are more Corona discharges, and a distorted wave shape of the first negative alternation induced voltage, showing much more energy losses, the Ls Cs circuit oscillation is first strongly asymmetric; up to when Corona discharges are finished. The starting slope of the discharge current is very abrupt.

3.1.5 Discharge with Uo = 100 Volts (1.033 Joule)

— Peak Current = 579 Amperes.

— Peak to peak output voltage Vpp = **56000 Volts**.

— Peak negative charge of Cs Vp = **— 42000 Volts**. Larger than insulation voltage of Cs.

— Oscillating frequency = 7576 Hertz.

— Recorded on file TEK0048.jpg. (Figure 11).

— Energy efficiency: $h = Cs / C1 (Vp / Uo)^2$ = **2033 %**.

— Energy efficiency 300 µs later = **20.3 %. Energy losses = 2033 – 20,3 = 2013 %**

Relative energy losses are increasing when the discharge Voltage is increased.

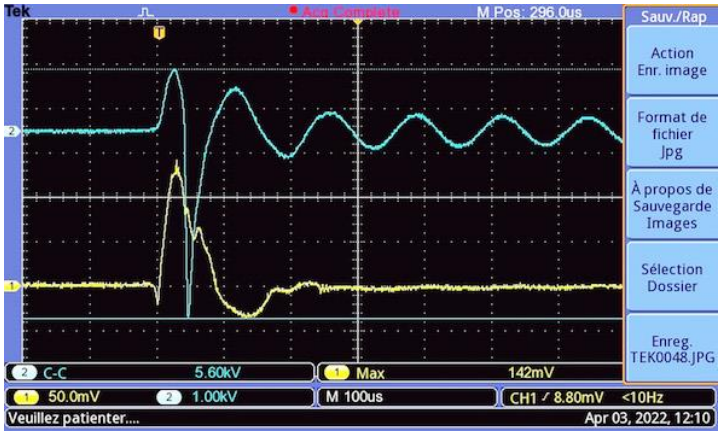

Figure 11. Discharge with Uo = 100 Volts. Yellow curve = discharge current (204 Amperes per division). Blue curve = induced voltage Vpp (10000 Volts per division). Time scale = 100 µs per division.

3.2 Summary of Energy Efficiencies at End of Discharges

Input energy E1 stored into capacitor C1 is equal to: $E1 = 1/2\ C1\ Uo^2$ (1)

Output energy Es charged into capacitor Cs at peak Voltage Vp is equal to: $Es = 1/2\ Cs\ Vp^2$ (2)

Energy efficiency with value of Vp is equal to: $h = Cs / C1\ (Vp / Uo)^2 = 1{,}153 . 10^{-4}\ (Vp / Uo)^2$ (3)

Energy efficiency with value of Vpp is: $h = ¼\ Cs / C1\ (Vpp / Uo)^2 = 2{,}88 . 10^{-5}\ (Vpp / Uo)^2$ (4)

Therefore:

— Energy efficiency type (4) of 40 Volts discharge is **373 %**.

— Energy efficiency type (3) of 40 Volts discharge is **460 %**.

— Energy efficiency type (4) of 60 Volts discharge is **402 %**.

— Energy efficiency type (3) of 60 Volts discharge is **508 %**.

—Energy efficiency type (4) of 80 Volts discharge is **577 %**.

— Energy efficiency type (3) of 80 Volts discharge is **1037 %**.

— Energy efficiency type (4) of 100 Volts discharge is **904 %**.

— Energy efficiency type (3) of 100 Volts discharge is **2033 %**.

3.3 Summary of Energy Efficiencies 300 µs After Beginning of Discharges

When we consider the peak to peak voltage Vpp at time 300 µs after the start of the discharge (central white line into de oscillograms), where induced voltage shape become symmetric, using again relation (4), we get:

— Energy efficiency Type (4) 300 µs after 40 Volts discharge with Vpp(300) = 10000 Volts, h = **180 %**.

— Energy efficiency Type (4) 300 µs after 60 Volts discharge with Vpp(300) = 12200 Volts, h = **119 %**.

— Energy efficiency Type (4) 300 µs after 80 Volts discharge with Vpp(300) = 10600 Volts, h = **51 %**.

— Energy efficiency Type (4) 300 µs after 100 Volts discharge with Vpp(300) = 8400 Volts, h = **20.3 %**.

This in spite of evident Corona discharges losses into remaining air bubbles into capacitor Cs and Ls coil.

Effectively, the four values of Vpp(300) are almost equal. Which means there are Corona discharges losses, into tiny air bubbles remaining into coil Ls, and into capacitor Cs because Paschen driven gas discharges stop at similar electric fields. At that time we did not vacuum impregnate such kinds of circuits with oil. Improvement was made later with an adequate oil recipient and generator concept.

3.4 Evolution of Peak Current Versus Uo Voltage of Discharges

During Uo = 40 Volts discharge, peak current Ip is 183 Amperes, therefore ratio Uo / Ip = **0.219** Ohm.

During Uo = 60 Volts discharge, peak current Ip is 290 Amperes, therefore ratio Uo / Ip = **0.207** Ohm.

During Uo = 80 Volts discharge, peak current Ip is 408 Amperes, therefore ratio Uo / Ip = **0.196** Ohm.

During Uo = 100 Volts discharge, peak current Ip is 579 Amperes, therefore ratio Uo / Ip = **0.173** Ohm.

This means emitter EM278 **does not follows Ohm's law**. When the charge voltage Uo increases by a factor 2.5, the energy by a factor 6,25, the peak current increases by a factor 3.164. This means it increases like $Uo^{1.257}$.

The discharge current ***derivative*** should be proportional to the peak current value, because current rise time duration remains almost the same (18 µs), so it should also increase like $Uo^{1.257}$. ***This seems to justify the larger than 100 % induction efficiency***. We will check that later.

Theoretically, without magnetic transformer core saturation, the global energy efficiency should be proportional to the square of the transformer coils ratio (111^2) and it should also be proportional to the square of the discharge current derivative. This means it should be proportional to $Uo^{2.514}$. Here it increases less than that, which means the transformer core gets briefly saturated for the largest peak currents.

3.5 Replication, and Results of Same Experiments With a Not Superconducting Device (Control)

We checked that the previous results were reproducible with emitter EM278. They were also similar with other emitters (EM273, EM277) of the same composition, but smaller total area. The maximum measured efficiency increased with emitter area.

We have also replicated the same experiments with a normally conducting device (control), made of a stack of metal plates. During these control discharges, we observed constant lower than 100 % energy efficiencies, when Uo value was changed from 40 to 100 Volts. And with control, the peak discharge current was proportional to Uo (Ohm's Law).

4. Discussion

4.1 There Must Be an External Energy Source

Energy conservation intangible principle forbids the possibility to get larger than 100 % energy efficiencies into such electric circuits. The control discharges made into a normally conducting device reinforce that principle.

Consequently, ***there must be another source of energy*** acting onto the circuit, to explain our reproducible systematic results with emitter EM278. That other energy source acts only onto emitter EM278, because it is only by replacing it by a control, that there is no more energy efficiency larger than 100%.

4.2 Hypotheses About the Observed Effects

We have already reported [Poher, 2011, 2] & [Poher, 2017, 4] that same external energy extraction effect when studying the propelling effect created by similar emitters, as the propelling momentum was proportional to the electric energy sent to the same kind of emitters. Effectively, this fact means that the propelling kinetic energy is proportional to the SQUARE of the powering electric energy of emitters. This also would be impossible without the action of an external energy source.

The only available external energy source here ***is the natural Quantum Field, cause of Gravitation***, interacting permanently with the superconducting matter of our emitters. We have studied that phenomenon previously, both experimentally and theoretically [Poher, 2011, 2], [Poher, 2020, 3], [Poher, 2017, 4], [Poher, 2020, 5].

Therefore here again, our emitters ***extract kinetic energy*** from that general Quantum field. ***There is a push of the internal free electrons as well as of Cooper pairs of electrons into the emitters***, which increase the peak discharge current, ***and particularly the discharge current derivative***. This is manifestly the cause of the larger than 100% energy efficiencies observed. We have checked that by measuring *the discharge current derivative*.

5. Current Derivative During Brief Electric Discharges Into Graphite Based Superconducting Emitters

5.1 Theoretical Introduction

We have proposed a Quantum model [Poher, 2020, 3] of Inertia from hypotheses. This model supposes the existence of a huge, ***isotropic***, general field of Gravitational Quanta, propagating at relativistic velocity *c* and carrying each a tiny constant momentum $Pu = 2.8.10^{-31}$ kg.m/s. When interacting with massive elementary matter particles, each Gravitational Quantum (named "Universon" instead of "Graviton) transfers briefly its momentum to the matter particle. That interaction is quite brief ($\tau = 7.8.10^{-14}$ second apparently), after which the Quantum recovers its freedom and previous momentum. The hypothetical phenomenon is similar to a brief time delay, or phase shift of the Quantum wave function.

According to calculated consequences of these hypotheses, when a massive matter particle is *at rest or has a constant velocity*, the permanent interaction with Gravitational Quanta ***has no effect*** onto the matter particle movement and mass, and has no effect onto the space distribution of Gravitational Quanta trajectories. ***This means their flux remains locally isotropic***.

In contrast, when the massive matter particle ***is accelerated***, the output flux of briefly interacting Quanta ***is no more isotropic***, the flux intensity is doubled in the direction of the matter particle acceleration, into a minuscule solid angle value proportional to the matter particle acceleration.

This prediction seems to be the cause of second Newton's Law: *Force = Mass times Acceleration*.

Effectively, the massive matter particle is propelled by the anisotropic quanta emission, like a rocket, ***in the opposed direction of the increased jet of output quanta***, this means in the opposed direction of the particle acceleration. This because particle and quanta momentum conservation.

We have checked and confirmed those hypotheses experimentally [Poher, 2011, 2], [Poher, 2020, 3], [Poher, 2017, 4] and [Poher, 2020, 5]. More than that, our theoretical model explains apparently the enigmatic

gravitational behavior of matter into galaxies, into clusters of galaxies, and during several cosmological observed facts [Poher, 2020, 3]. ***This without dark matter hypothesis***.

It is impossible to observe that same phenomenon by accelerating electrons into ***normal conductors*** by an electric field, because the electric field accelerates positive ions in the reverse directions, so the anisotropies created by each kind of accelerated particles (electrons and ions) cancel each other.

According to BCS model of superconductors [Cooper, 1956, 10], [Bardeen, 1957, 11], electrons associate into interlinked pairs into such materials (Cooper pairs), which are accelerated by electric fields, with positive ions vibrating **in perpendicular planes** versus the acceleration direction of these pairs.

This seems to be the reason why our emitters of a Gravitational field ***must be made of superconducting material and Josephson Junctions*** into this material, in order to be able to accelerate strongly Cooper pairs of electrons.

We confirmed experimentally the predicted propelling effect of emitters during electric discharges, without ejection of matter particles [Poher, 2011, 2].

We can even suppose that Cooper pairs of electrons, into the superconducting material, aggregate, like bosons, into very brief Bose-Einstein condensates, during their very brief electric field accelerations (This being suggested by tight current derivative slope).

Here, we want to check the effect of anisotropic re-emission of Gravitational Quanta onto the discharge current derivative into our circuits.

According to our Quantum model of Inertia, accelerated Cooper pairs of electrons re-emit an ***anisotropic*** flux of Gravitational Quanta (Universons), into a superconducting material.

That anisotropic flux ***accelerates ALL matter particles it interacts with***. This is a very short distance phenomenon, with a random distribution of internal Josephson Junctions axes, and electric fields, into the superconducting material, at nanometer scale.

The anisotropic re-emission of Gravitational Quanta pushes and accelerates all free electrons. That acceleration is not caused by an electric field, it should increase the total number of accelerated electrons, (the discharge current intensity should increase) so the energy storage capacitor should be discharged ***faster*** than into normal conductors.

This means the discharge current derivative should be increased. This derivative should increase the Faraday's induction into the transformer. But electric energy into the primary discharge circuit should remain the same, only kinetic energy of the discharge electrons should be increased. ***That phenomenon has been effectively reported [Poher, 2017, 4]. But let us measure it***.

5.2 Theoretical Value of the Discharge Current Derivative

The primary circuit of the transformer, in Figure 1, is a classical RLC circuit with capacitor C1 initially charged at voltage Uo. The discharge current I(t) into such a circuit follows a differential equation:

$$1 / C1 \int I(t)\, dt \text{ — } Lp\ \partial I / \partial t + Rp\ I(t) = Uo \qquad (5)$$

Where Lp and Rp are the total distributed inductance and resistance of the primary circuit.

At instant t = 0 of discharge beginning, discharge current I(0) is nil, so the current derivative should be maximum and defined by:

$$\partial I / \partial t\ (t = 0) = \text{ — } Uo / Lp \qquad (6)$$

Distributed inductance Lp is made of the L1 inductance of the primary coil, plus the distributed inductance of the conductors (about one µH per meter length), plus the internal inductance of all components C1, Thyristor, and Emitter. We can calculate the value of Lp ***from the discharge current rise time*** revealed by oscillograms of Figures 6, 7, 8 and 18, as this rise time is constant and equal theoretically to $(Lp\ C1)^{½}$.

Figure 18, observed at time scale of 25 microseconds per division, shows that $(Lp\ C1)^{1/2} = 32$ µs.

Therefore, with C1 = 206.5 µF, we get Lp = 4.96 µH.

Applying expression (6), we get the four **theoretical** successive peak values of the discharge current derivatives we should have observed with the four successive values of Uo:

— During discharge Uo = 40 Volts, theoretical ∂I / ∂t (t = 0) = **8.066** Amperes per micro second.

— During discharge Uo = 61 Volts, theoretical ∂I / ∂t (t = 0) = **12.3** Amperes per micro second.

— During discharge Uo = 80 Volts, theoretical $\partial I / \partial t$ (t = 0) = **16.13** Amperes per micro second.

— During discharge Uo = 101 Volts, theoretical $\partial I / \partial t$ (t = 0) = **20.37** Amperes per micro second.

5.3 Fabrication and Calibration of a Current Derivative Probe for Oscilloscope Measurements

We built a specific oscilloscope probe to measure the real discharge current derivative.

That probe was made from a Rogowski coil (Figure 12), where Faraday's induction into that coil is proportional to the derivative of the magnetic field created by an electric current. Illustrations show the probe fabrication and installation.

Figure 12. 250 turns Rogowski probe coil

The Rogowski coil support is an isolated copper cable of 4.5 mm diameter and 80 mm length. The coil is made of 250 contiguous turns of 0.28 mm diameter enamelled copper wire. Its total length is 70 mm.

One of the coil terminals is soldered to the internal copper wire of the support, to get the coil terminals on the same end (Figures 13 & 14 & 15).

We measured the electrical characteristics of that Rogowski probe before soldering it to a coaxial cable:

— Resistance in direct current = 1.10 Ohm.

— In alternative current at100 Hertz, inductance = 14 μH, resistance = 1.24 Ohm.

— In alternative current at 1000 Hertz, inductance = 13.9 μH, resistance = 1.241 Ohm.

— In alternative current at 10000 Hertz, inductance = 13.59 μH, resistance = 1.272 Ohm.

— In alternative current at 100000 Hertz, inductance = 11.433 μH, resistance = 2.025 Ohms.

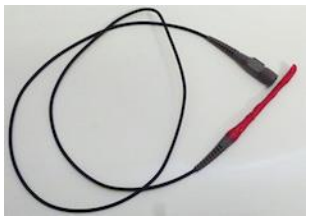

Figure 13. Rogowski coil soldered to an oscilloscope compatible coaxial cable and tape insulated

Figure 14. Rogowski probe, winded around an extension brass conductor

Figure 15. Rogowski probe bolted onto Figure 7 discharge circuit black box negative terminal

The coaxial cable itself has an internal resistance of 270 Ohms, which increases the probe resistance. The time constant L/R of the probe at 10000 Hertz frequency is therefore 0.05 μs with coaxial cable, which is adequate for observing the real discharge current derivative.

5.4 Calibration of the Current Derivative Probe

We used a professional Chauvin Arnoux MA 200 current probe, surrounding the discharge current conductor, and a graphical method for measuring the current derivative and calibrate this way our new probe. The MA200 current probe was used with 10 mV per Ampere sensitivity, and saturation for 400 peak Amperes. Three calibration discharges were made.

5.4.1 Calibration Discharge With Uo = 47 Volts (0.228 Joule) Into Emitter EM278 and Coil L1

— Peak current from MA200 = 2160 mV or 216 peak Amperes.

— Derivative probe peak voltage = 896 mV.

— Recorded as TEK 0005.jpg. (Figure 16).

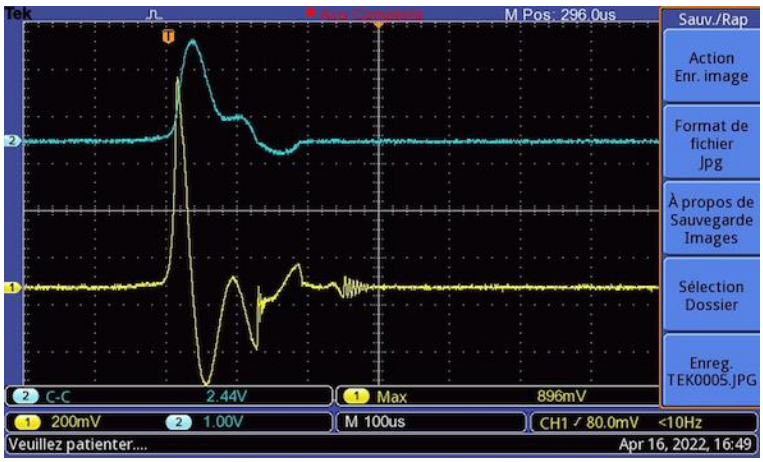

Figure 16. Discharge II-4-A with Uo = 47 Volts. Yellow curve = discharge current derivative (200 mV per division). Blue curve = discharge current (100 amperes per division). Time scale = 100 μs per division

The yellow signal from our new probe is apparently showing a correct wave shape. It culminates where the discharge current slope (blue color) is maximum, it is positive for an increasing current and vice-versa, it is nil where the current slope changes sign. We have printed that oscillogram and measured graphically the current maximum slope: **10.81 Amperes per μs**.

This corresponds to a peak signal value of 896 mV from our probe, which means 10.81 A/μs for 896 mV.

The first value of the calibration factor is therefore **82.89 mV per A/μs**.

5.4.2 Calibration Discharge With Uo = 66 Volts (0.45 Joule) Into Emitter EM278 and Coil L1

— Peak current from MA200 = 3200 mV or 320 peak Amperes.

— Derivative probe peak voltage = 1400 mV.

— Recorded as TEK 0006.jpg. (Figure 17).

— Peak slope of current = 18.61 A/µs

— Second calibration factor = **75.27 mV per A/µs**.

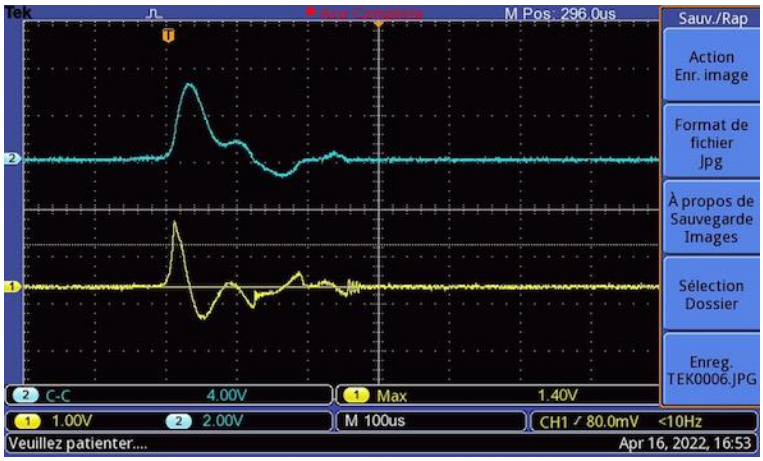

Figure 17. Discharge II-4-B with Uo = 66 Volts. Yellow curve = discharge current derivative (1000 mV per division). Blue curve = discharge current (200 amperes per division). Time scale = 100 µs per division

5.4.3 Calibration Discharge With Uo = 60 Volts (0.372 Joule) Into Emitter EM278 and Coil L1

— Peak current from MA200 = 2880 mV or 288 peak Amperes.

— Derivative probe peak voltage = 1240 mV.

— Recorded as TEK 0008.jpg. (Figure 18).

— Peak slope of current = 14.81 A/µs

— Third calibration factor = **83.73 mV per A/µs**.

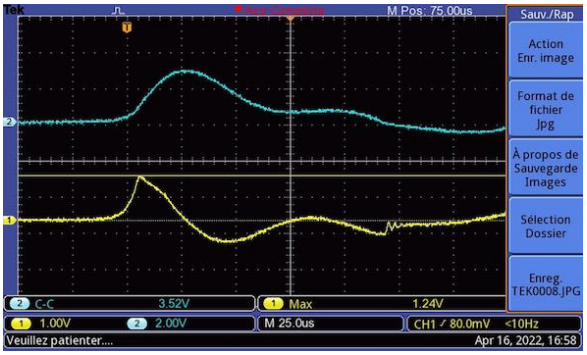

Figure 18. Discharge II-4-C with Uo = 60 Volts. Yellow curve = discharge current derivative (1000 mV per division). Blue curve = discharge current (200 amperes per division). Time scale = 25 µs per division

<u>Average calibration factor of our probe</u> = (82.89 + 75.27 + 83.73) / 3 = <u>80.63 mV per A/µs</u>.

5.5 Comparison of Theoretical and Measured Current Derivatives With Emitter EM278

For this comparison, channel #2 of oscilloscope measures induced voltage Vpp(t) to be multiplied again by 10, and channel #1 is connected to our new discharge current derivative probe. Four similar discharges as figures 8 to 11 were made.

5.5.1 Discharge With Uo = 40 Volts (0.1652 Joule) Into Emitter EM278 and Coil L1

— Peak to peak induced voltage Vpp = 14000 Volts.

— Derivative probe peak voltage = 760 mV. This means **9.426 A/µs**

— Recorded as TEK 0001.jpg. (Figure 19).

— Peak energetic efficiency = **353 %**.

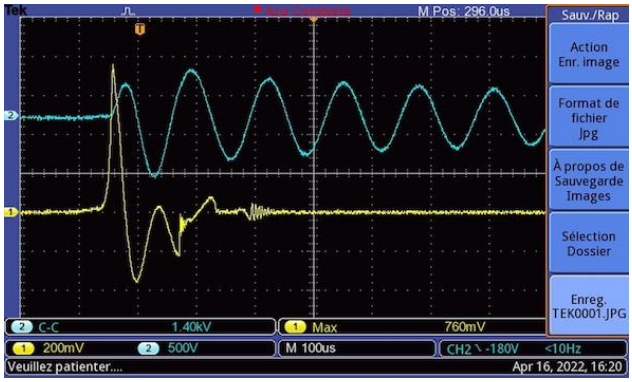

Figure 19. Discharge II-5-D with Uo = 40 Volts. Yellow curve = discharge current derivative (200 mV per division). Blue curve = induced voltage Vpp (5000 Volts per division). Time scale = 100 µs per division.

5.5.2 Discharge With Uo = 61 Volts (0.3842 Joule) Into Emitter EM278 and Coil L1

— Peak to peak induced voltage Vpp = 23200 Volts.

— Derivative probe peak voltage = 1320 mV. This means **16.371 A/µs**

— Recorded as TEK 0002.jpg. (Figure 20).

— Peak energetic efficiency = **417 %**.

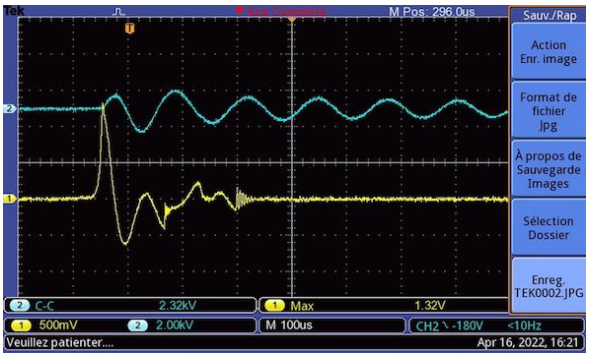

Figure 20. Discharge II-5-E with Uo = 61 Volts. Yellow curve = discharge current derivative (500 mV per division). Blue curve = induced voltage Vpp (20000 Volts per division). Time scale = 100 µs per division.

5.5.3 Discharge With Uo = 80 Volts (0.66 Joule) Into Emitter EM278 and Coil L1

— Peak to peak induced voltage Vpp = 36000 Volts.

— Derivative probe peak voltage = 1840 mV. This means **22.82 A/µs**

— Recorded as TEK 0003.jpg. (Figure 21).

— Peak energetic efficiency = **583 %**.

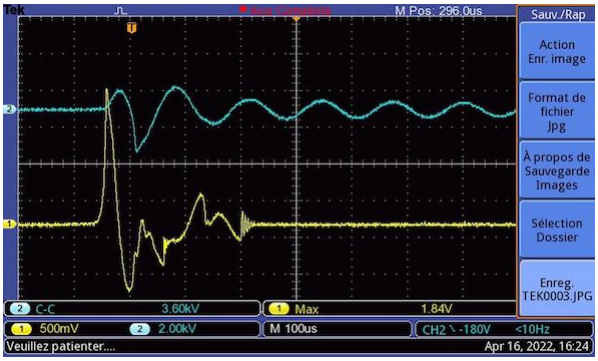

Figure 21. Discharge II-5-F with Uo = 80 Volts. Yellow curve = discharge current derivative (500 mV per division). Blue curve = induced voltage Vpp (20000 Volts per division). Time scale = 100 µs per division

5.5.4 Discharge With Uo = 101 Volts (1.05 Joule) Into Emitter EM278 and Coil L1

— Peak to peak induced voltage Vpp = 56000 Volts.

— Derivative probe peak voltage = 2440 mV. This means **30.262 A/µs**

— Recorded as TEK 0004.jpg. (Figure 22).

Peak energetic efficiency = **885 %**.

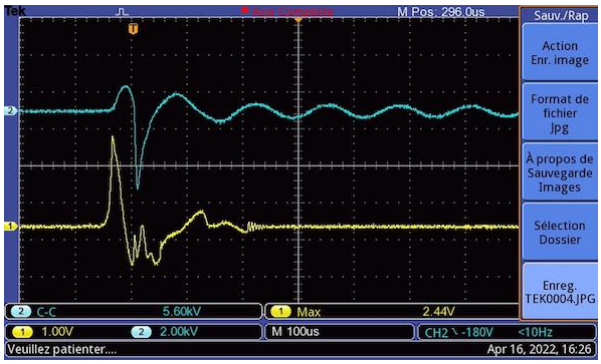

Figure 22. Discharge II-5-G with Uo = 101 Volts. Yellow curve = discharge current derivative (1000 mV per division). Blue curve = induced voltage Vpp (20000 Volts per division). Time scale = 100 µs per division

Anomalies of current derivatives wave shapes observed during discharges F and G mean a brief saturation of the magnetic material ***and Corona effect discharges***. This reduces a bit energy efficiency.

It is interesting to consider peak to peak largest range of discharge current derivatives:

- In D: 13.83 A/µs.
- In E: 24.41 A/µs.
- In F: 34.73 A/µs.
- In G: 43.31 A/µs.

5.5.5 Summary of Current Derivative Measurements

Let us draw Table 1:

Table 1

Uo (1)	Input Joules (2)	Energy Efficiency % (3)	Vpp (Volts) (4)	Derivative peak A/µs (5)	Δ total derivative (6)	Ratio (3)/(5)	Ratio (4) / (6)	Ratio (4) / (5)	Ratio (3) / (6)	Ratio $(6)^2/(3)$	Ratio $(5)^2/(3)$
40 V	0.1652	353 %	14000	9.426	13,83	37.45	1012.3	1485	25.52	0.542	0.25
61 V	0.3842	417 %	23200	16.371	24,41	25.47	950.4	1417	17.1	1.43	0.642
80 V	0.66	583 %	36000	22.82	34,73	25.55	1036.6	1578	16.79	2.07	0.893
101 V	1.05	885 %	56000	30,262	43.31	29.24	1293	1850	20.43	2.12	1.035

From Table 1 experimental results, several properties are deduced:

— Column of ratios (3) / (5) shows that there is not a simple correlation between energy efficiency and peak value of current derivative, most probably because of magnetic saturation.

— Column of ratios (4) / (6) shows that peak to peak induced voltage Vpp(t) is almost proportional to the peak to peak current derivative variation during a discharge.

— As well, column of ratios (4) / (5) shows that peak to peak induced voltage Vpp(t) is almost proportional to peak current derivative (Faraday's law).

— Column of ratios (3) / (6) shows that energy efficiency increases less than peak to peak current derivative variation during a discharge.

— Column of ratios $(6)^2$ / (3) shows that energy efficiency increases less than peak to peak current derivative variation during a discharge

— Column of ratios $(5)^2$ / (3) shows that energy efficiency increases less than square of peak current derivative variation during a discharge. This confirms magnetic saturation.

Let us now draw table II of ratios (5) / (1), (6) / (1) et (3) / (1). From Table 1 results.

Table 2

Charge voltages Uo (1)	Peak derivative ratios (5) / (1)	Total derivative range ratios (6) / (1)	Ratio of Energy efficiencies (3) / (1)
40 V	**0.236**	**0.346**	**8.825**
61 V	**0.268**	**0.400**	**6.836**
80 V	**0.285**	**0.434**	**7.288**
101 V	**0.299**	**0.429**	**8.762**

Ratios in Table 2 mean that peak current derivative increases 1.267 times while the charge voltage Uo of capacitor C1 increases 2.525 times.

As well, peak to peak range of current derivative increases 1.24 times while charge voltage Uo of capacitor C1 increases 2.525 times.

<u>This confirms that Emitter EM278 does not follows Ohms law.</u>

This is the reason why peak to peak induced voltage increases by a factor 4 while charge voltage Uo of capacitor

C1 increases by a factor 2.525, which means 1,584 times more.

And finally energetic efficiency increases almost proportionally to charge voltage Uo.

6. Comparison of Current Derivative Measurements With Theoretical Values of Current Derivatives

Remember: applying theoretical expression (6), we should observe the four following **theoretical** successive peak values of the discharge current derivatives:

— During discharge Uo = 40 Volts, theoretical $\partial I / \partial t (t = 0)$ = **8.066** Amperes per micro second.

— During discharge Uo = 61 Volts, theoretical $\partial I / \partial t (t = 0)$ = **12.3** Amperes per micro second.

— During discharge Uo = 80 Volts, theoretical $\partial I / \partial t (t = 0)$ = **16.13** Amperes per micro second.

— During discharge Uo = 101 Volts, theoretical $\partial I / \partial t (t = 0)$ = **20.37** Amperes per micro second.

With our new oscilloscope probe we have measured the **REAL** following current derivatives:

— During discharge Uo = 40 Volts, a peak current derivative of **9.426** A / µs. This is **1.1686 times more**.

— During discharge Uo = 61 Volts, a peak current derivative of **16.371** A / µs. This is **1.331 times more**.

— During discharge Uo = 80 Volts, a peak current derivative of **22.82** A / µs. This is **1.415 times more**.

— During discharge Uo = 101 Volts, a peak current derivative of **30.262** A / µs. This is **1.486 times more**.

It is therefore quite clear that the primary circuit behavior is very different than the one described by theoretical differential equation (5). ***Evidently emitter EM278 is the cause of that fact***.

7. What Happens Inside Emitter EM278?

From Figure 1 diagram, it is clear that only the emitter can be the cause of an energy efficiency larger than 100%. This is never observed when replacing the emitter by a normal conductor (control). And it is the considerable increase of the induced voltage Vpp(t) which allows the observed large energy efficiencies. They are calculated the following way:

$$\eta = 1/4 \,.\, Cs / C1 \,.\, (Vpp / Uo)^2 = 2.88 \,.\, 10^{-5} (Vpp / Uo)^2 \qquad (7)$$

The transformer coils ratio is 111/1 turns, so when applying briefly 80 Volts to the primary coil we should observe less than 8880 peak output Volts. Here we observe 25540 peak output Volts. This means 2.877 times more. and it is Faraday's induction which creates Vpp(t).

Theoretically the induced voltage into secondary coil Ls is proportional to the derivative of the magnetic induction existing inside the transformer magnetic core. This means that the induced voltage into secondary coil Ls is proportional to the derivative of the discharge current crossing primary coil L1.

So the brief increase of the discharge current derivative, created by the emitter, is the cause of the larger than 100 % energy efficiency. ***The emitter increases the current discharge derivative of C1 into L1***.

Consequently, capacitor C1 is discharged faster when there is an emitter in the discharge circuit.

The number of electrons circulating each microsecond, into the emitter, is strongly increased, because free electrons are not only accelerated by the electric field, ***they are also pushed and accelerated strongly by the anisotropic Quantum Gravitational flux***, re-emitted by the electrically accelerated Cooper pairs of electrons. These exist into the Josephson Junctions of the emitter superconducting material. This is the way our theoretical model justifies the observed facts.

The push of electrons is what ***increases really the discharge current derivative*** as measured by our new probe into Figures 6, 7, 8, 9, 10, 11 and 12, where the peak derivative values are observed about 5 µs after the discharge beginning, when the accelerating electric field, and the current value are still simultaneously large.

It is while the accelerating electric field is the largest, and the number of accelerated Cooper pairs number is also the largest, that the intensity of the anisotropic re-emission of gravitational Quanta is the strongest, increasing the electrons push, and increasing simultaneously the discharge current derivative. This is coherent.

The emitter **extracts kinetic energy** from the general isotropic Quantum flux cause of Gravitation, which interacts permanently with its particles. It is only during the brief and strong acceleration of electrons Cooper pairs, inside the emitter, that kinetic energy is mainly extracted and transferred to the electrons.

This is what predicts our Inertia and Gravitation Quantum model [Poher, 2020, 3]. And this is not a weak kind of phenomenon, because this is Inertia, not gravity.

Now let us apply these increased energy experimental results to an electric generator concept.

8. Application to a Concept of Patented Prototypes of Gravitational Electric Energy Generators

From previous results, we proposed a concept of Autonomous electric Generators, extracting their energy from the general natural quantum Gravitational field. Here is the generator concept typical diagram:

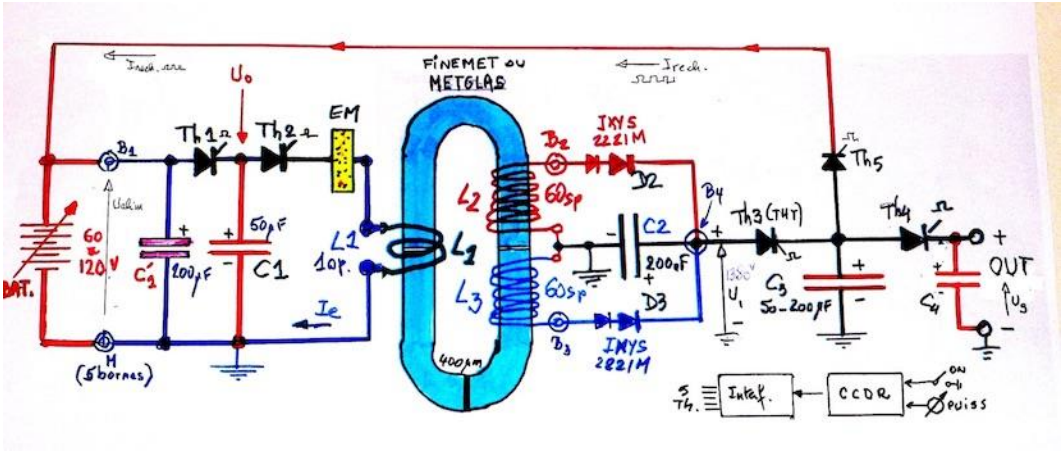

Figure 23. Electric circuit diagram of an autonomous electric Quantum Gravitational Generator prototype

Into this concept there are two similar induced secondary coils Ls named L2 and L3 and two Diodes named D2 and D3, this in order to get a two alternations AC to DC energy conversion into Cs named now C2. The primary discharge circuit is the same as in Figure 1, except that there is now a battery charging C1 through a capacitive energy transfer between C'1 and C1 when thyristor Th1 is conducting.

Discharges into the primary circuit through the emitter are made when thyristor Th2 is conducting. So that circuit works exactly as explained previously.

An output set of several thyristors Th3, Th4, Th5, and capacitors C3 and C4 are added at the output side of the basic energy generation circuit.

8.1 Sequence of the Five Non GTO Thyristors Firing and Generator Functioning

All thyristors are controlled by a micro controller and its software, installed into an electronic sub-system named CCDR (Command and Control of Discharges and Regulation). This subsystem controls the gates / cathodes voltages of all thyristors through electronic interfaces and pulse transformers.

The CCDR software commands the very brief thyristors conduction repetitively in sequence:

- First, Th1 charges C1 from Battery voltage Uo with a parallel capacitor C'1 allowing high frequency repetition (up to 2000 Hertz). This charge has a duration of about 100 µs.
- Then Th2 discharges C1 into the one turn primary coil L1 through emitter EM. This has a duration of about 200 µs.
- A same high AC voltage is induced into the two secondary coils L2 and L3, which are rectified by high Voltage Diodes D2 and D3. The DC charge of capacitor C2 is full along about 100 µs.
- Then high voltage thyristor Th3 is activated briefly in order to transfer the electric energy stored into capacitor C2 to capacitor C3 at a much lower voltage, compatible with the user needs.
- Then output energy is alternatively transferred to the user through thyristor Th4 OR to the battery recharge circuit through thyristor Th5. *Recharge could also be made through a L4 secondary coil.*
- Then the sequence returns to the beginning, after a manually or automatically ***controlled time delay*** defining the frequency of discharges repetition rate and average generator power. About 2000 Hertz at full power, and as slow as one hertz.
- ***The discharges repetition frequency is effectively what controls the generator average electric power.***

8.2 Practical Implementation of the Generator Concept Prototype

Figure 24. We first immerged high voltage circuits into a stainless steel recipient allowing vacuum evacuation of air bubbles into the coils and Cs capacitor plates, and used our hexagonal shape emitter.

Figure 25. Vacuum evacuation of air bubbles into the immersed circuits.

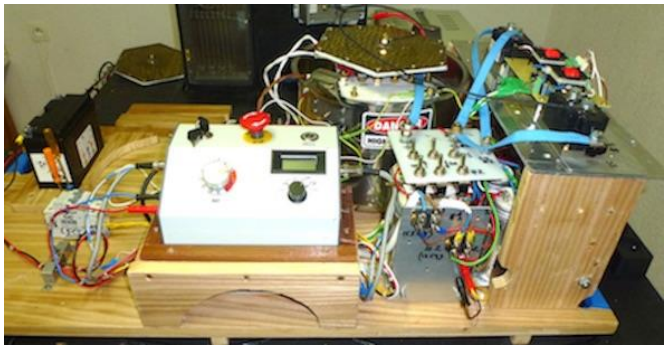

Figure 26. Practical implantation of Generator prototype. All high voltage circuits are immersed into mineral oil with vacuum evacuation of air bubbles causing Corona discharges energy losses. White box is the CCDR. Large currents conductors are insulated Copper braids.

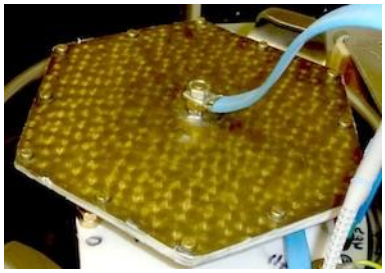

Figure 27. Emitter EM280 used into the generator prototype has a hexagonal shape.

The use of a rechargeable battery defining voltage Uo is required in order to stabilize the generator power control trough a PID based software, because the generator global energy efficiency is proportional to the input Uo voltage. The PID software sampled control loop would effectively stop it, or diverge and saturate the power, if Uo voltage was not stabilized. Other methods of Uo stabilization than batteries are of course also possible.

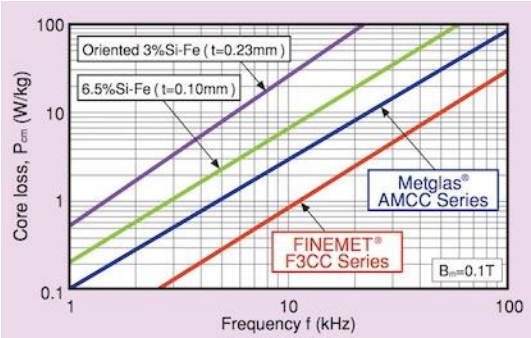

Figure 28. We use Finemet C core magnetic material for low energy losses at the oscillation frequency

With that generator prototype we tested the ability of repeating the discharges at different frequencies as well as the long duration reproducibility of performances.

Figure 29. Compact implementation of high voltage circuits of the generator prototype for oil immersion

8.3 Examples of Experimental Results Obtained With Generator Prototype

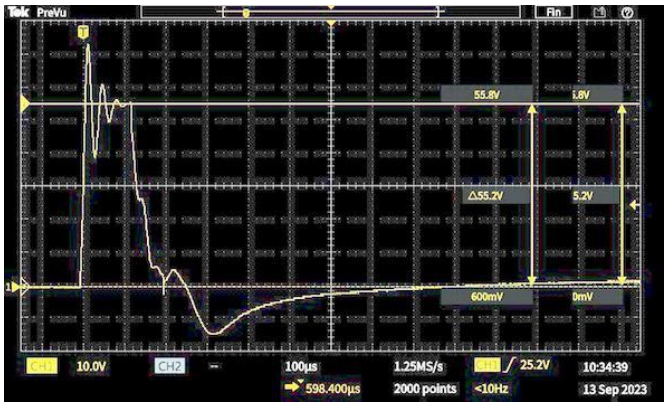

Figure 30. Evolution of Uo voltage charging C1 = 50 µF when battery is replaced by a 62 Volts DC laboratory 300 Watts power supply, during successive firings of Thyristors Th1 and Th2.

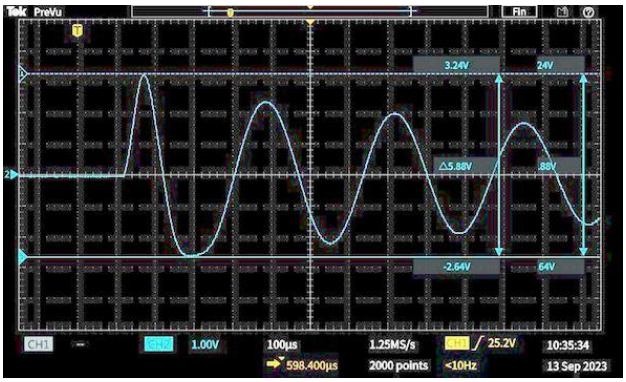

Figure 31. Evolution of induced voltage across L2 during Figure 26 discharge with Uo = 55.8 volts. We measured, through a 1/1000 compensated voltage divider, + 3240 Volts and — 2640 Volts (5880 Volts peak to peak). **This means 1378 % peak energy efficiency**.

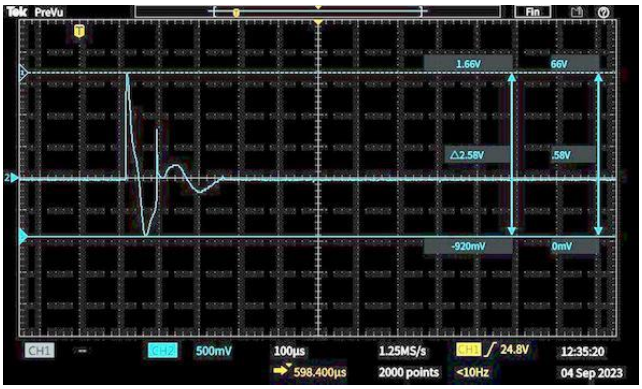

Figure 32. Evolution of discharge current derivative during the Uo = 55.8 Volts discharge. We measured 20,84 million Amperes per second peak.

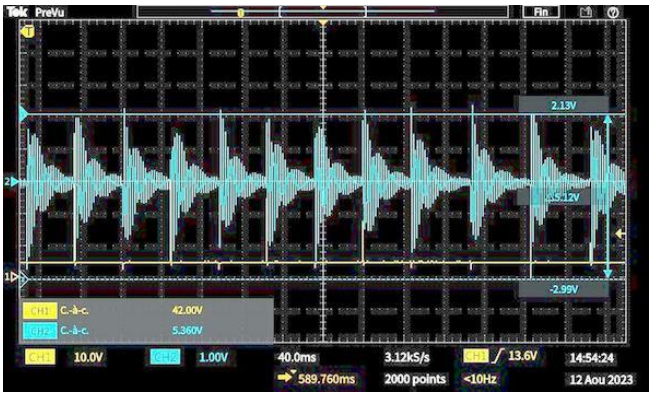

Figure 33. Evolution of induced voltage across L2 during about 20 Hertz discharges repetition frequency

9. Conclusion

We demonstrated theoretically and experimentally larger than 100 % energy efficiencies during discharges into patented “Emitters” made of partially superconducting Graphite, associated with adequate transformers and electric circuits. Our emitters interact with the general Quantum field cause of Gravitation. They extract kinetic energy from that field, at Quantum level.

From our results, we proposed concepts of prototype Autonomous Gravitational Electric Generators.

We are proposing that concept to potential industrial partners, hopefully for Exploitation Licensing of our intellectual property, and international patents, for replication and tests at larger power levels, and for mass production.

Such generators seem to be able to replace most of the electric batteries, into electric vehicles, in the near future.

They should give an infinite range to these vehicles, with no need for recharge, and should allow travelling at nil cost per kilometer after initial investment.

They do not emit any greenhouse gases, and create no pollution, so they should contribute to improve Earth climate evolution, if generalized.

Emitters, and their applications to generation of electric energy, as well as other kinds of predicted applications, have been internationally patented into many industrially advanced countries.

Acknowledgments

Authors thank the editor and their anonymous referees for their revision suggestions.

Authors’ contributions

Claude POHER = CP — Danielle POHER = DP — Conceptualization, CP. ; Methodology, CP, DP.; Software, CP.; Validation, CP, DP.; Formal Analysis, CP, DP.; Investigation, CP, DP.; Resources, CP,DP.; Data Curation, CP,DP.; Writing CP,DP. – Original Draft Preparation, CP.; Writing – Review & Editing, CP,DP.; Visualization, CP, DP.; Supervision, CP.; Project Administration, CP.; Funding Acquisition, CP, DP.

Funding

The two authors have both privately financed that research without any participation from an external source.

Competing interests

The authors declare that they have no known competing financial interests or personal relationships that could have appeared to influence the work reported in this paper.

Informed consent

Obtained.

Ethics approval

The Publication Ethics Committee of the Canadian Center of Science and Education.

The journal and publisher adhere to the Core Practices established by the Committee on Publication Ethics (COPE).

Provenance and peer review

Not commissioned; externally double-blind peer reviewed.

Data availability statement

The data that support the findings of this study are available on request from the corresponding author. The data are not publicly available due to privacy or ethical restrictions.

Data sharing statement

No additional data are available.

References

Bardeen, J., Cooper, L. N., & Schrieffer, J. R. (1957). *Phys. Rev., 108*, 1175-1204. https://doi.org/10.1103/PhysRev.108.1175

Cooper, L. N. (1956). Bound electron pairs in a degenerate Fermi gas. *Physical Review, 104*(4), 1189-1190. Bibcode:1956PhRv..104.1189C. https://doi.org/10.1103/PhysRev.104.1189

Esquinazi, P. (2019). Ordered defects: A roadmap towards room temperature Superconductivity and Magnetic order. Retrieved from https://arxiv.org/abs/1905.07489v1

Josephson. (1974). The discovery of tunnelling supercurrents. *Rev. Mod. Phys., 46*(2), 251–254. https://doi.org/10.1103/RevModPhys.46.251

Kopelevich, Y., Esquinazi, P., Torres, J. H. S., & Moehlecke, S. (1999). Ferromagnetic- and Superconducting-like Behavior of Graphite. Retrieved from https://arxiv.org/pdf/ cond-mat/9912413.pdf

Poher, C. (2006). Europ Patent publication WO 2007/093 699 A2, PCT FR 2007/000249 (February 14, 2006). Retrieved from https://www.epo.org/searching-for-patents.html

Poher, C. (2011). Physical phenomena observed during strong electric discharges into layered Y123 superconducting devices at 77 K. *Applied Physics Research, 3*(2), 51. https://doi.org/10.5539/apr.v3n2p51

Poher, C., & Modanese, G. (2017). Enhanced induction into distant coils by YBCO and silicon-graphite electrodes under large current pulses. *Physics Essays, 30*(4). https://doi.org/10.4006/0836- 1398-30.4.435

Poher, C., & Poher, D. (2020). Gravity & matter Quantum behavior, from accelerations, during electric discharges into Graphite- based superconductor. https://doi.org/10.5539/apr.v12n2p48

Poher, C., & Poher, D. (2020). Quantum model of Inertia – Predictions - Confirmations, Consequences for Gravitation into galaxies, and CDM Cosmology models. https://doi.org/10.5539/apr.v12n2

Rubin, V. (1995). A Century of Galaxy Spectroscopy. *The Astrophysical Journal, 451*, 419ff. Bibcode:1995ApJ...451..419R. https://doi.org/10.1086/176230

Scheike, T., Böhlmann, W., Esquinazi, P., Barzola-Quiquia, J., Ballestar, A., & Setzer, A. (2012). Can doping graphite trigger room temperature superconductivity? Evidence for granular high-temperature superconductivity in water-treated graphite powder. [cond- mat.supr-con]— *JETP Letters, 100*, 336(2014). Retrieved from https://arxiv.org/abs/1209.1938